OPEN

Polarization response of nanowires *à la carte*

Alberto Casadei[1], Esther Alarcon Llado[1], Francesca Amaduzzi[1], Eleonora Russo-Averchi[1], Daniel Rüffer[1], Martin Heiss[1], Luca Dal Negro[2,3] & Anna Fontcuberta i Morral[1]

[1]Laboratoire des Matériaux Semiconducteurs, Institut des Matériaux, École Polytechnique Fédérale de Lausanne, CH-1015 Lausanne, Switzerland, [2]Department of Electrical and Computer Engineering and Photonics Center, Boston University, 8 Saint Marys Street, Boston, MA, 02215, USA, [3]Division of Materials Science and Engineering, Boston University, 15 Saint Marys Street, Brookline, MA 02446, USA.

Thanks to their special interaction with light, semiconductor nanowires have opened new avenues in photonics, quantum optics and solar energy harvesting. One of the major challenges for their full technological deployment has been their strong polarization dependence in light absorption and emission. In the past, metal nanostructures have been shown to have the ability to modify and enhance the light response of nanoscale objects. Here we demonstrate that a hybrid structure formed by GaAs nanowires with a highly dense array of bow-tie antennas is able to modify the polarization response of a nanowire. As a result, the increase in light absorption for transverse polarized light changes the nanowire polarization response, including the polarization response inversion. This work will open a new path towards the widespread implementation of nanowires applications such as in photodetection, solar energy harvesting and light emission.

S emiconductor nanowires (NWs) provide an extraordinary platform for nano-optoelectronic applications, including lasers[1], optical switching[2], solar cells[3–6] and photo-detectors[7,8]. The reduced dimensions in NWs lead to the possibility of manipulating light-matter interactions at the nanoscale. Through the tuning of the NW morphological parameters and substrate composition, devices with controlled photonic and electrical properties can be designed[9,10]. By combining semiconductor NW dielectric properties and optically resonant metal nanoparticles one can further enhance and localize light absorption[11–16].

It is well-known that nanowires exhibit a highly anisotropic polarization response both in light absorption and emission: light absorption occurs preferentially for light polarization along the NW axis, with some dependence on the diameter[17,18]. This means that a nanowire lying on a substrate responds mostly to light polarized along its axis, and it is almost transparent for light polarized perpendicular to the NW axis. Thus, almost half of all incoming white light passes through a NW without interacting. This anisotropy limits the use of NWs in some photonic applications, such in photodetectors and solar cells[9]. Previous studies have studied the optical coupling between disk-shaped nanoantennas and one-dimensional structures[19,20]. Some evidence of polarization dependent response have been reported in second harmonic generation and Raman scattering. While Raman scattering is increased in diminutive structures such as carbon nanotubes[20], the electric field enhancement was only observed in the infrared region for larger diameter structures such as GaAs nanowires[19]. Moreover, these studies did not involve any deliberate engineering of the absorption spectra or absorption rate. In this work, we design a plasmonic antenna to directly counteract the characteristic anisotropic polarization response of GaAs nanowires, without diminishing the absorption rate of light polarized along the nanowire. This enables us to modify the NW polarization response up to the point of inversion and to enhance the NW absorption in the visible spectrum. We also show the possibility to enhance light absorption up to 15 times in the infrared. This design principle is not restricted to the material of study and wavelengths under study; these principles can be extended to other materials and other regions of the electromagnetic spectrum. The large parameter space for light absorption design and the special opto-electrical properties of GaAs, such as a direct band-gap in the visible range, high absorption coefficient and high charge mobility, imply a very high potential of this platform for a multitude of nano-optoelectronic devices.

The proposed device is presented schematically in Fig. 1a. A nanowire is embedded in a bow-tie antenna array with a goal of engineering the nanowire polarization response. The nanoantennas dimensions were chosen to maximize the electric field inside the nanowire (Supplementary Information 1), which corresponded to a set
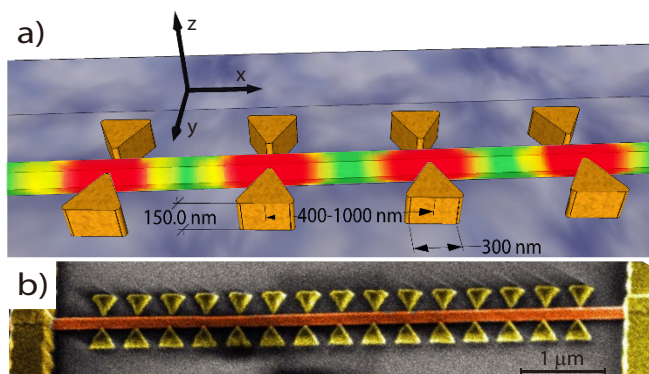
Figure 1 | (a) Scheme of the nanowire-nanoantenna system. The different colors in the NW are an illustrative representation of the field energy distribution inside the NW during the excitation of transverse polarized light. The red color indicates the highest field energy density and the green the lowest. (b) SEM image of a contacted NW embedded in a bow-tie nanoantennas array. The NW diameter is 150 nm and the distance between nanoantennas is $d = 400$ nm.

height and width of 150 and 300 nm respectively. These values are strictly linked to the nanowire diameter (150 nm) and they were designed to optimize the absorption of incident transverse polarized light. Additionally, for the bow-tie antennas to modify the light interaction with the NW, they have to be positioned as close as possible to the NW[19]. In our case, this nanoantenna/nanowire gap was as small as 10 nm, which corresponds to the finest fabrication precision available to us. An example of a fabricated device is shown in Fig. 1b. A GaAs nanowire with a diameter between 140 and 146 nm has been inserted in a dense bow-tie antenna array and contacted electrically to allow photoconductance measurements. In order to ensure an ohmic contact, a highly p-doped 40 nm shell (2×10^{18} cm^{-3}) was added[21]. All devices were fabricated on glass, however a different substrate would influence the overall shape of the response, though the bow-tie antennas would continue to tailor the NW polarization response. A glass substrate is preferable over an oxidized silicon wafer because it reduces the occurrence of possible light interference effects[22].

For light polarized along the axis, the bow-tie antennas provide a strong confinement of the incident light in their gap[23]. By positioning a dielectric NW in the gap, the antenna resonances should result in an increase of light absorption in the NW. In order to verify this hypothesis, we calculated the corresponding light absorption and field energy distribution in a single NW, in bow-tie antenna arrays and in a hybrid nanowire/bow-tie antenna system. The results of these calculations are shown in 2. Fig. 2a shows the normalized calculated absorption spectra of a GaAs nanowire with a diameter of 150 nm and hexagonal cross-section for light perpendicular to the nanowire axis. Absorption tends to decrease for longer wavelengths, with two absorption peaks at 500 and 680 nm. These peaks are related to photonic resonances in the NW and have been studied extensively in the literature[24,25]. Figure 2b depicts the intensity of light within the nanowire cross-section in these resonant cases. The NW acts as a cavity, leading to enhanced light absorption with respect to an equivalently thick film. The field energy distribution profile and the in plane electric field lines indicate the presence of the TE_{01} and TE_{11} coupled modes[26] (supplementary information 2). Figure 2c corresponds to the field energy calculations on the bow-tie antenna arrays for a varying inter-antenna distance. In order to represent the capacity of the antennas to concentrate the light, the electric field intensity is integrated on the volume corresponding to the NW in the nanowire/nanoantennas system. Overall, the capacity of the antennas to concentrate light increases when they are closely spaced. Interestingly, there are certain wavelengths for which this concen-

tration is remarkably enhanced. For example, for an inter-antenna distance of 550 nm, one observes resonances at 660 and 770 nm. The resonances move spectrally as a function of the inter-antenna distance due to their capacitive coupling. Fig. 2d plots the square of the electric field across the antenna gap for these resonances. Light is mostly concentrated in the gap region closest to the antennas. Fig. 2e shows the absorption spectrum of the full nanowire when sandwiched between a bow-tie antenna array, as a function of the inter-antenna distance. At large inter-antenna distances, the absorption in the nanowire is barely affected. By bringing the antennas closer together, the absorption is enhanced in the spectral region between 650 and 840 nm following the antenna modes (Fig. 2c). If one looks now at the profile of the absorption modes in the NW for an inter-antenna distance of 550 nm, one can see that only the intensity of modes $\alpha 1$ and $\beta 1$ has changed. Interestingly, at $\lambda = 840$ nm, the nanoantennas generate an absorption enhancement in the NW of 15 times. This enhanced mode $\gamma 3$ exhibits an intensity profile similar to what it is expected from the antenna geometry (Supplementary information 3).

We turn now to the experimental demonstration of the coupling of the bow-tie antenna modes with a NW. Absorption in the nanowire/bow-tie antenna system has been obtained by photoconductivity measurements. We have fabricated devices with various inter-antenna distances: 1000 and 400 nm. Figures 3a–c and d–f respectively show the predicted absorption and experimental photoconductivity spectra of nanowires for polarizations along and across the NW axis. Fig. 3a shows the photoconductivity spectra of a single nanowire. As expected, we predict higher absorption for wavelengths close to 500 nm and 650 nm, corresponding to the existence of optical guided modes. Absorption is significantly higher for polarization parallel to the nanowire axis, a consequence of the one-dimensional shape of the nanowire[18,27]. As shown in Fig. 3b, the polarization anisotropy is suppressed by the addition of bow-tie antennas with $d = 1000$ nm. Interestingly, this suppression is broad-band and is valid from 500 to 900 nm. By bringing the antenna closer together (400 nm) it is possible to favor light absorption for light polarized perpendicular to the nanowire axis, at least for the spectral range between 600 and 750 nm.

As shown in Figs. 3d–f, we are able to experimentally observe the predicted switched anisotropic absorption through photocurrent measurements in real devices. Thanks to the addition of the bow-tie nanoantennas close to the nanowire, it is possible to concentrate the incoming light and thereby increase the photo-current related to light polarized across the nanowire axis. Interestingly, light absorption can be enhanced up to a factor 3.6 with respect to a single NW in the spectral region between 650 and 750 nm. In contrast, the absorption for longitudinal polarized light is not significantly modified. While the simulated absorption efficiency values can be quantitatively compared between all device configurations, a direct comparison of photo-current absolute values between different real devices is not accurate. Small variations in the nanowire diameter and distance between the contacts result in slight changes in the photoconductance and measured photocurrent. For this reason, we report in figures 3d, 3e and 3f the absolute values of the photocurrent. More than two devices have been fabricated for each design and the results are consistent.

We have demonstrated the possibility to control and engineer the polarization response of nanowires through the coupling with a bow-tie antenna array. Absorption of transverse polarized light can be enhanced up to 15 times and photoconductivity measurements have been performed on the fabricated devices. Calculations and measurements show that bow-tie nanoantennas behave like a dipole antennas and, when excited with transverse polarized light, they couple plasmonically with the NW. The nanowire/bow-tie antenna platform gives the opportunity to engineer devices that respond in different ways when excited by optical light. The adaptability and control of
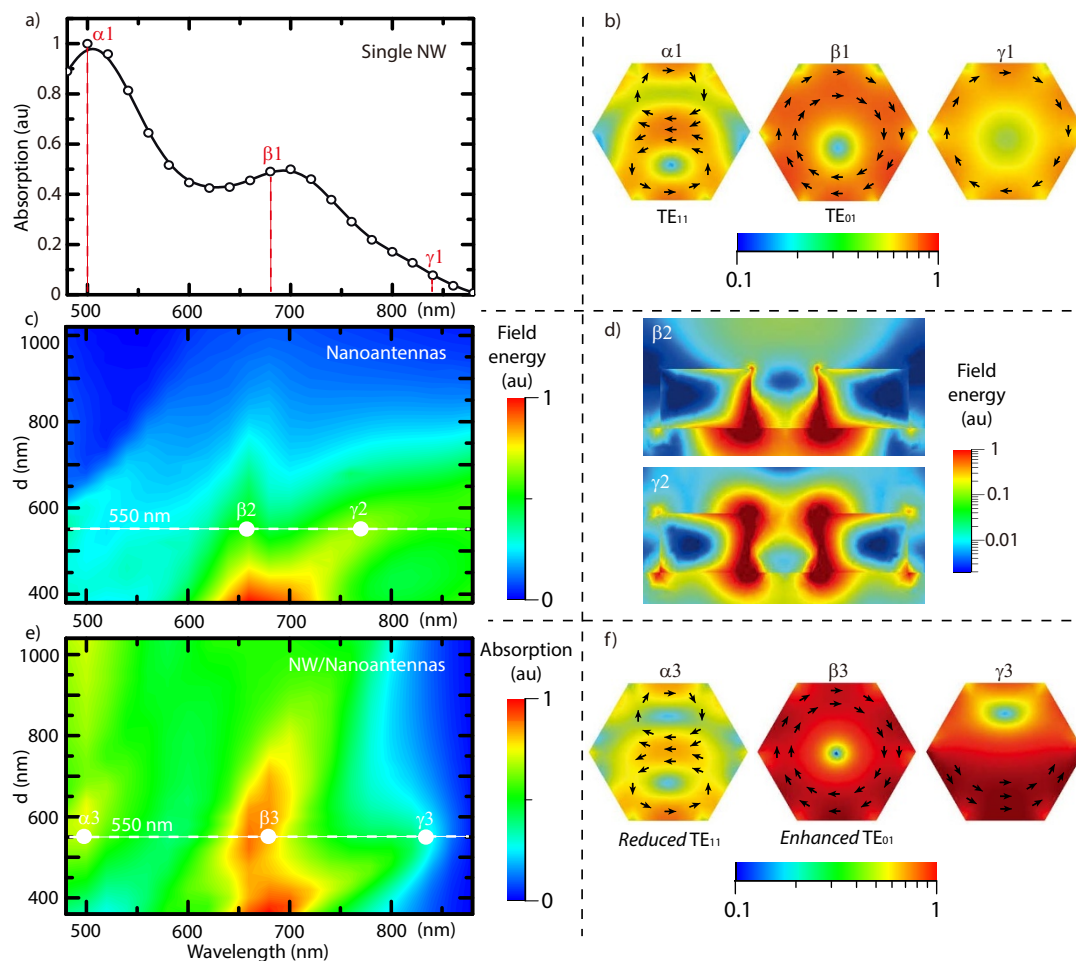
Figure 2 | (a) Calculated absorption spectra of a GaAs nanowire with a diameter of 150 nm in diameter lying on a glass substrate. For the points α1, β1 and γ1 the electric field intensity and the electric field lines are represented along the NW cross section in (b). (c) Calculated field energy map for an array of gold antennas on glass as a function of the wavelength and the inter-nanoantenna distance d. (d) Field energy distribution in the plane along the antennas axis corresponding to the points β2 and γ2. (e) Calculated absorption map for the nanowire/nanoantenna system on a glass substrate as a function of the nanoantenna distance d. The corresponding α3, β3 and γ3 electric field intensity and in-plane electric field lines are shown in (f). All the calculations were performed with light incident on the plane at perpendicular angle and transversely polarized with respect to the NW axis.
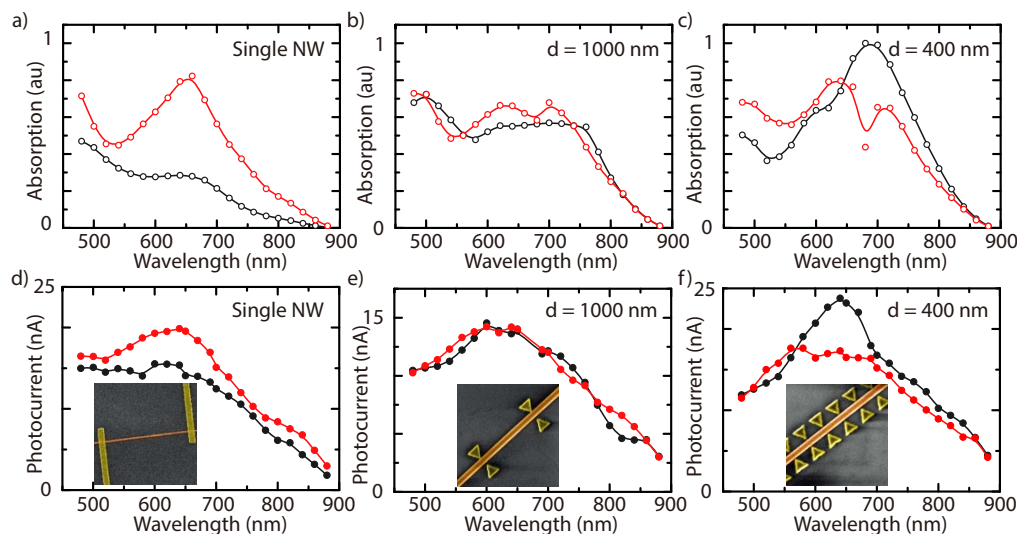
Figure 3 | Calculated absorption efficiency spectra of a single NW (a) and nanowire/nanoantennas systems with antenna distance $d = 1000$ (b) and $d = 400$ nm (c). The black points correspond to the calculation for light perpendicular to the NW axis and the red points for light parallel to the NW axis. (d), (e) and (f) represent the electrical photo-current measurements of the corresponding above calculations obtained with laser power of 10 μW. The lines between the data points are guides for the eyes. In the insets, the scanning electron microscopy images of the analyzed devices are shown.

this design makes the NW/nanoantenna platform an optimal candidate for engineering nano-scale opto-electronic devices like solar cells, photo-detectors, optical switches, optical emitters and modulators.

Methods

Nanowire growth. GaAs NWs were grown with an intrinsic core and a p-doped shell under conditions described elsewhere[21], leading to a diameter of around 145 nm and a length of approximately 12 μm. In this work the p-type doping was achieved by adding a flux of carbon during the growth of the shell in order to reach a doping concentration of $2 \cdot 10^{18}$ cm^{-3} [21]. NWs present mainly a zinc blend crystal structure with few twins per μm and a small tapering leading to around 10 nm of difference between the bottom and top diameter.

Device fabrication. The devices were prepared by transferring NWs to a fused silica substrate and their position was localized by using an optical microscope. The nanoantennas have been designed around the NWs using a custom-made fitting software. The pattern encodes the relative position on the wafer and uses circular shapes for deep sub-micron alignment. The position is determined via shape recognition algorithms leading to an accuracy between 50 and 10 nm. We used electron beam lithography (Vistec EBPG5000) to position the nanoantennas in close proximity to the NW surface and along its axis. Before the exposure, a MMA and PMMA resist layer were spin coated on the substrate and the evaporation of 40 nm of Cr was needed in order to dissipate the electrons coming from the electron beam. The Cr was then etched away and the evaporation of 5 nm of Ti and 150 nm of Au was performed after the developing of the resist. The electrical contacts consist of Pd/Ti/Au (40/10/200 nm) metal layer in contact with the NW doped shell leading to ohmic contacts[28].

Photocurrent measurements. The photo-conductivity measurements are performed with two point measurements by applying a constant voltage and continuously measuring the current with a picoammeter/voltage source (Keythey 6487). A superK Koheras continuum laser is used to excite the devices with monochromatic light. The excitation beam is focused on the NW/nanoantenna system to a spot size of approximately 5 μm by a 50× objective (NA 0.5). The power is set constant for all the wavelengths to 10 μW leading to a power density of 50 W/cm^2. An optical polarizer is used to change the light polarization and a CCD camera is used to control the location of the incident light on the sample. During the data acquisition a power supply applies a constant voltage of 50 mV and measures the current between the NW contacts.

1. Saxena, D. *et al.* Optically pumped room-temperature GaAs nanowire lasers. *Nature Photonics* **7**, 963–968 (2013).
2. Piccione, B., Cho, C.-H., van Vugt, L. K. & Agarwal, R. All-optical active switching in individual semiconductor nanowires. *Nature Nanotechnology* **7**, 640–645 (2012).
3. Krogstrup, P. *et al.* Single-nanowire solar cells beyond the Shockley–Queisser limit. *Nature Photonics* **7**, 306–310 (2013).
4. Wallentin, J. *et al.* InP nanowire array solar cells achieving 13.8% efficiency by exceeding the ray optics limit. *Science* **339**, 1057–1060 (2013).
5. Kelzenberg, M. D. *et al.* Enhanced absorption and carrier collection in Si wire arrays for photovoltaic applications. *Nature Materials* **9**, 239–244 (2010).
6. Tian, B. *et al.* Coaxial silicon nanowires as solar cells and nanoelectronic power sources. *Nature* **449**, 885–890 (2007).
7. Hayden, O., Agarwal, R. & Lieber, C. Nanoscale avalanche photodiodes for highly sensitive and spatially resolved photon detection. *Nature Materials* **5**, 352–356 (2006).
8. Dai, X. *et al.* GaAs/AlGaAs nanowire photodetector. *Nano Letters* **14**, 2688–2693 (2014).
9. Heiss, M. & Fontcuberta i Morral, A. Fundamental limits in the external quantum efficiency of single nanowire solar cells. *Applied Physics Letters* **99**, 263102 (2011).
10. Tchernycheva, M. *et al.* Integrated Photonic Platform Based on InGaN/GaN Nanowire Emitters and Detectors. *Nano Letters* **14**, 3515–3520 (2014).
11. Mokkapati, S. *et al.* Polarization tunable, multicolor emission from core–shell photonic III–V semiconductor nanowires. *Nano Letters* **12**, 6428–6431 (2012).
12. Mokkapati, S., Saxena, D., Tan, H. H. & Jagadish, C. Design considerations for semiconductor nanowire-plasmonic nanoparticle coupled systems for high quantum efficiency nanowires. *Small* **9**, 3964–3969 (2013).
13. Mann, S. A. & Garnett, E. C. Extreme light absorption in thin semiconductor films wrapped around metal nanowires. *Nano Letters* **13**, 3173–3178 (2013).
14. Mühlschlegel, P., Eisler, H.-J., Martin, O. J. F., Hecht, B. & Pohl, D. W. Resonant Optical Antennas. *Science* **308**, 1607–1609 (2005).
15. Novotny, L. & van Hulst, N. Antennas for light. *Nature Photonics* **5**, 83–90 (2011).
16. Bharadwaj, P., Deutsch, B. & Novotny, L. Optical Antennas. *Advances in Optics and Photonics* **1**, 438–483 (2009).
17. Wang, J., Gudiksen, M. S., Duan, X., Cui, Y. & Lieber, C. M. Highly polarized photoluminescence and photodetection from single indium phosphide nanowires. *Science* **293**, 1455–1457 (2001).
18. Chen, G. *et al.* Optical antenna effect in semiconducting nanowires. *Nano Letters* **8**, 1341–1346 (2008).
19. Casadei, A. *et al.* Photonic-plasmonic coupling of GaAs single nanowires to optical nanoantennas. *Nano Letters* **14**, 2271–2278 (2014).
20. Heeg, S. *et al.* Plasmon-enhanced raman scattering by carbon nanotubes optically coupled with near-field cavities. *Nano Letters* **14**, 1762–1768 (2014).
21. Casadei, A. *et al.* Electrical transport in C-doped GaAs nanowires: surface effects. *physica status solidi RRL* **7**, 890–893 (2013).
22. Colombo, C., Krogstrup, P., Nygård, J. L., Brongersma, M. & Fontcuberta i Morral, A. Engineering light absorption in single-nanowire solar cells with metal nanoparticles. *New Journal of Physics* **13**, 123026 (2011).
23. Forestiere, C. *et al.* Genetically Engineered Plasmonic Nanoarrays. *Nano Letters* **12**, 2037–2044 (2012).
24. Cao, L. *et al.* Engineering light absorption in semiconductor nanowire devices. *Nature Materials* **8**, 643–647 (2009).
25. Huang, Y. F., Chen, C. Y., Chen, L. C., Chen, K. H. & Chattopadhyay, S. Plasmon management in index engineered 2.5D hybrid nanostructures for surface-enhanced Raman scattering. *NPG Asia Materials* **6**, e123 (2014).
26. Bures, J. *et al.* Guided optics. (Wiley-VCH, Weinheim, 2009).
27. Bronstrup, G. *et al.* A precise optical determination of nanoscale diameters of semiconductor nanowires. *Nanotechnology* **22**, 385201 (2011).
28. Casadei, A. *et al.* Doping incorporation paths in catalyst-free Be-doped GaAs nanowires. *Applied Physics Letters* **102**, 013117 (2013).

Author contributions

E.R.A., M.H. and D.R. contributed to the NWs growth. A.C. fabricated the samples, performed the experiments and analyzed data. E.A.L. and A.C. carried out the simulations. F.A. participated in the discussions and performed the Raman spectroscopy studies. A.C., E.A.L. and A.F.iM. wrote the manuscript in collaboration with all the authors. A.F.iM. and A.C. conceived the experiment. L.D.N. participated in the discussions and in the writing of the manuscript. A.F.iM. planned the set of experiments and supervised the project. All authors have given approval to the final version of the manuscript.

Additional information

Supplementary information accompanies this paper at http://www.nature.com/scientificreports

Competing financial interests: The authors declare no competing financial interests.

How to cite this article: Casadei, A. *et al.* Polarization response of nanowires à la carte. *Sci. Rep.* **5**, 7651; DOI:10.1038/srep07651 (2015).